Detection and analysis of angiogenesis pathway-associated lncRNA expression profiles in human skin fibroblasts under high-glucose conditions

LONGXIANG TU[1], QIN HUANG[2], YANGHONG HU[3] and DEWU LIU[1]

Departments of [1]Burns Surgery and [2]Nursing, The First Affiliated Hospital of Nanchang University; [3]Department of Nursing, Jiangxi University of Traditional Chinese Medicine, Nanchang, Jiangxi 330006, P.R. China

Received September 23, 2019; Accepted June 22, 2020

DOI: 10.3892/mmr.2020.11333

Abstract. Accumulating evidence has indicated that long non-coding RNAs (lncRNAs) have crucial roles in wound healing and that vascular lesions in diabetic wounds are frequently difficult to heal. However, the role of angiogenesis pathway-associated lncRNAs in wound healing in diabetic patients has remained to be fully elucidated. In the present study, human skin fibroblasts were cultured under high-glucose conditions *in vitro* to mimic a diabetic environment and the angiogenesis pathway-associated lncRNA expression profile in the high- and normal-glucose groups was examined. The microarray data indicated that 14 lncRNAs and 22 mRNAs were differentially expressed. Several candidate lncRNAs and mRNAs were then analyzed by reverse transcription-quantitative PCR and the results were consistent with the microarray data. Furthermore, the University of California Santa Cruz Genome Browser was used to identify mRNAs linked to angiogenesis pathways near the transcriptional region of lncRNAs. The results suggested that lncRNAs RP4-791C19.1 and CTD-2589O24.1 may act on their target genes epidermal growth factor receptor and p21 (RAC1) activated kinase 1, respectively, as enhancers and cis-regulate their expression. Therefore, the present study confirmed that several angiogenesis pathway-associated lncRNAs were differentially expressed under high-glucose conditions, which may have a key role in wound healing in patients with diabetes.

Introduction

With the population aging, the incidence of diabetes mellitus is gradually increasing (1). Diabetes may lead to various complications, among which foot ulcer is a major complication that may seriously affect the quality of life, lead to a prolonged hospital stay and may even result in lower limb amputation (2). Vascular lesions in diabetes are difficult to heal due to impaired angiogenesis and deregulated vascular homeostasis (3).

Long non-coding RNAs (lncRNAs), a class of non-coding RNAs longer than 200 nucleotides regulate gene expression at multiple levels, including epigenetic regulation, transcriptional regulation and post-transcription regulation (4). Emerging evidence has indicated that lncRNAs also have crucial roles in the development and progression of skin wound healing (5). lncRNA5322 may promote the proliferation and differentiation of hair follicle stem cells by targeting the microRNA (miR)-21-mediated PI3K/AKT signaling pathway in these cells (6). Overexpression of lncRNA AC067945.2 is able to reduce collagen expression in skin fibroblasts through vascular endothelial growth factor (VEGF) and Wnt signaling pathways (7). lncRNA X-inactive specific transcript (XIST) is inversely regulated by miR-29a and overexpression of lncRNA XIST in denatured dermis may promote human skin fibroblast proliferation and migration, as well as extracellular matrix synthesis (8). Previous studies have confirmed that lncRNAs are closely linked to angiogenesis (9). However, the role of angiogenesis pathway-associated lncRNAs in wound healing in diabetes has remained largely elusive.

In the present study, human skin fibroblasts were cultured under high-glucose conditions *in vitro* to mimic a diabetic environment and angiogenic pathway-associated lncRNA expression profiles were compared between the high and normal glucose groups. Several candidate angiogenesis pathway-associated lncRNAs and mRNAs were analyzed by reverse transcription-quantitative PCR (RT-qPCR). In addition, the University of California Santa Cruz (UCSC) Genome Browser was used to identify lncRNAs and their potential target mRNAs in the angiogenic pathway.

Materials and methods

Isolation of human fibroblasts and cell culture. The present study was approved by the Biomedical Ethics Committee of the Affiliated Hospital of Nanchang University (Nanchang, China). Written informed consent was obtained from all patients. Human skin tissues were obtained from the remaining

Correspondence to: Professor Dewu Liu, Department of Burns Surgery, The First Affiliated Hospital of Nanchang University, 17 Yongwai Street, Nanchang, Jiangxi 330006, P.R. China
E-mail: dewuliu@126.com

Key words: fibroblasts, long non-coding RNA, angiogenesis

skin samples of three patients (one female who was 25 years old; two males, age, 20-32 years) who underwent skin grafting at the Department of Burns Surgery of the First Affiliated Hospital of Nanchang University (Nanchang, China) between January 2016 and June 2018. During this time period, the skin cells were isolated from fresh tissues, and only the skin cells were one patient were cultured at a time.

The tissues were washed three times with PBS and a penicillin/streptomycin solution (Beijing Solarbio Science and Technology Co., Ltd.). The tissues were subsequently cut into 10x10 mm sections and were digested with 0.25% trypsin + EDTA (Gibco; Thermo Fisher Scientific, Inc.) at 4˚C for 8 h. Dulbecco's modified Eagle's medium (DMEM) with glucose (5.5 mM) supplemented with 10% fetal bovine serum (FBS; GE Healthcare) was added to terminate the digestion. The epidermis was removed with tweezers and the dermal tissues were rinsed with PBS and sliced into small pieces (0.5-1 mm^3). The tissue pieces were then placed on a 25-cm^2 Petri dish (Corning, Inc.) to which 5 ml of culture medium containing DMEM with glucose (5.5 mM) supplemented with 100 U/ml penicillin plus 100 mg/ml streptomycin and 10% FBS were added. The dish was then placed in an incubator containing air with 5% CO_2 and saturated humidity at 37˚C. The culture medium was replaced every 3 days. The fibroblasts exhibited fusion after 14 days and were then sub-cultured on a 25-cm^2 Petri dish. The subsequent experiments were performed with third-generation fibroblasts. Fibroblasts ($2x10^5$) that were seeded on 6-well plates were subjected to different treatments: Fibroblasts cultured in conditioned medium with 5.5 mM glucose were used as the control group and fibroblasts cultured in conditioned medium with 50 mM glucose were used as the experimental group. Each group was set up in three wells. After 48 h of culture, the total RNA was extracted.

RNA extraction and quality control. Total RNA was isolated with TRIzol reagent (Invitrogen; Thermo Fisher Scientific, Inc.) according to the manufacturer's protocol. A NanoDrop ND-1000 spectrophotometer (NanoDrop Technologies; Thermo Fisher Scientific, Inc.) was used to estimate RNA quantity. RNA integrity and genomic DNA contamination were assessed by standard denaturing agarose gel electrophoresis.

Microarray and data analysis. The Agilent Array platform 2100 (Agilent Technologies, Inc.) was employed for the microarray analysis. Sample preparation and microarray hybridization were performed according to the manufacturer's protocols. In brief, mRNA was purified from total RNA following the removal of ribosomal RNA with an mRNA-ONLY™ Eukaryotic mRNA Isolation kit (Epicentre). Subsequently, each sample was amplified and transcribed into fluorescent complementary (c)RNA using the Arraystar Flash RNA Labeling protocol. The labeled cRNAs were hybridized onto the LncPath™ Human Angiogenesis Array (8x15 K; Arraystar), which simultaneously detected the expression of 828 lncRNAs and their 251 potential coding targets associated with the angiogenic signaling pathway. After washing the slides, the arrays were scanned using the Agilent Scanner G2505C (Agilent Technologies, Inc.). The Agilent Feature Extraction software (version 11.0.1.1; Agilent Technologies, Inc.) was used to analyze the acquired array images. Quantile normalization and subsequent data processing were performed using GeneSpring GX software (version 12.1, Agilent Technologies, Inc.). Differentially expressed lncRNAs and mRNAs with statistical significance between the two groups were identified through volcano plot filtering. The differentially expressed lncRNAs and mRNAs between the two samples were identified through fold change filtering. Hierarchical clustering was performed to display the distinguishable lncRNA and mRNA expression pattern between the samples. The microarray analysis was performed with the assistance of KangChen Biotech. To detect the functions of the lncRNAs, the GENCODE annotation (version 21) was used (10). For analysis of the lncRNAs and their potential protein-coding gene targets in the angiogenic pathway, the UCSC Genome Browser was used to identify the mRNAs associated with angiogenic pathways near the transcriptional region of lncRNA (http://genomeucsc.edu/).

RT-qPCR. Total RNA was extracted from each group with TRIzol reagent (Invitrogen; Thermo Fisher Scientific, Inc.) and then reverse-transcribed using an RT Reagent kit (Thermo Fisher Scientific, Inc.) according to the manufacturer's protocol. lncRNA expression levels in each group were estimated by RT-qPCR using an ABI Q6 (Applied Biosystems; Thermo Fisher Scientific, Inc.). Certain candidate lncRNAs were validated by PCR. The primers used in the present study are listed in Table I. The total RNA (1 μg) was transcribed into cDNA. PCR was performed in a total reaction volume of 10 μl, including 5.0 μl of 2X Master Mix (Roche), 1.0 μl of cDNA template, 0.3 μl of PCR forward primer (10 mM), 0.3 μl of PCR reverse primer (10 mM) and 4.4 μl of double-distilled water. qPCR was performed using an initial denaturation step of 10 min at 95˚C, followed by 40 cycles of 15 sec at 95˚C and 60 sec at 60˚C. Each RT-qPCR was performed in triplicate and all of the samples were normalized to GAPDH. The relative expression levels of the candidate genes were calculated using the $2^{-\Delta\Delta Cq}$ method (11).

Statistical analysis. All statistical analyses were performed using the SPSS 17.0 software package (SPSS, Inc.). Unpaired Student's t-tests were used to analyze the differentially expressed lncRNAs or mRNAs obtained in the microarray and PCR. $P<0.05$ was considered to indicate statistical significance. The threshold value set to designate differentially expressed lncRNAs and mRNAs was a fold change of ≥1.2 ($P<0.05$).

Results

Morphological characteristics of human skin fibroblasts. Human skin fibroblasts were isolated from skin tissues and cultured in DMEM with 10% FBS and 1,000 mg/l glucose. Following 7 days of culture, it was possible to see the fibroblast cells that had migrated from the tissue pieces (Fig. 1A). The fibroblasts exhibited a long spindle-shaped morphology with larger cell bodies. Following 14 days of culture, the fibroblasts covered the majority of the surface area of the 25-cm^2 Petri dish (Fig. 1B). The experiments were performed with third-generation fibroblasts. No difference in cell morphology was observed between cells cultured under high and normal glucose conditions (Fig. 1C and D).

Table I. Primers used for reverse transcription-quantitative PCR.

Seqname	Gene symbol	Sequence (5'-3')	Annealing temperature (˚C)	Product length (bp)
-	GAPDH	F: AGAAGGCTGGGGCTCATT R: TGCTAAGCAGTTGGTGGTG	60	158
ENST00000407916	RP4-791C19.1	F: CCAAGGGCAGACAAGTTACAATG R: TGGGTTTAACAGATTCCAGTACTCC	60	121
ENST00000534518	CTD-2589O24.1	F: GCCATCGCCGCCAGTGTATGT R: GGTAAAAGTAGATGCAGTACCTGATA	60	58
NM_003377	VEGFB	F: GATCCGGTACCCGAGCAGT R: TTAGGTCTGCATTCACACTGGC	60	72
NM_000899	KITLG	F: ATGACCTTGTGGAGTGCGTGA R: CAGATGCCACTACAAAGTCCTTGA	60	150
NM_000602	SERPINE1	F: GGTGAAGACACACACAAAAGGTAT R: CTCCAAAACTGCTGAAACTACA	60	102

F, forward; R, reverse; VEGFB, vascular endothelial growth factor B; KITLG, KIT ligand; SERPINE1, serpin family E member 1.

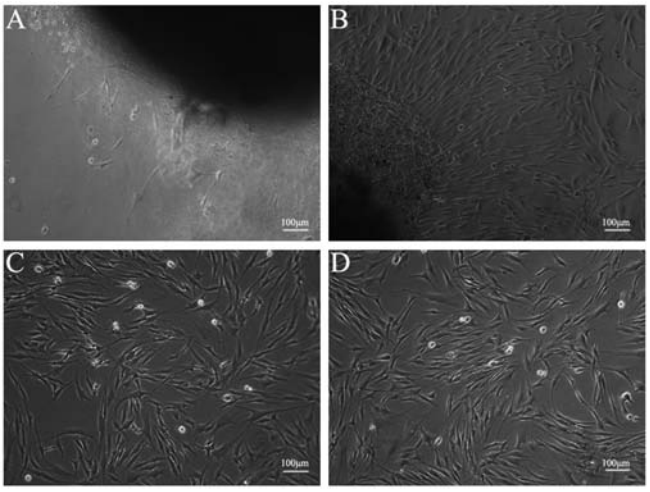

Figure 1. Morphological characteristics of human skin fibroblast under an inverted phase-contrast microscope. (A) Fibroblast derived from skin tissues cultured for 7 days; (B) fibroblasts derived from skin tissues cultured for 14 days. (C) Third-generation fibroblasts cultured under normal glucose conditions; (D) third-generation fibroblasts cultured under high-glucose conditions (scale bar, 100 μm).

RNA quantification and quality assurance. A NanoDrop ND-1000 spectrophotometer was used to accurately determine the quantity of RNA. The optical density at 260 nm (OD_{260})/OD_{280} ratios of total RNA were close to 2.0 for pure RNA and the OD_{260}/OD_{230} ratios of the total RNA samples were >1.8. RNA has a maximum absorption peak at a wavelength of 260 nm and proteins have a maximum wavelength of 280 nm (12). Therefore, the (OD_{260})/OD_{280} ratio was used to assess protein contamination, while the OD_{260}/OD_{230} ratio was used to assess organic compound contamination. The 18S and 28S ribosomal RNA bands, which were assessed using denaturing 1% agarose gel electrophoresis, were clearly visible in the RNA samples with an intensity ratio of ≥2:1. These results were in accordance with the requirements of the microarray analysis.

Overview of lncRNA profiles. Using microarray analysis, the angiogenesis pathway-associated lncRNA expression profiles of human skin fibroblasts under high glucose conditions were obtained (Figs. 2 and 3). The box plot reflects the gene expression data before and after standardization of the original data. After normalization, the median of the overall data were at the same level, indicating that the results of the data normalization were good (Fig. 2A and B).

Hierarchical cluster analysis is used to determine similarities between data for classification and is more commonly used in gene chip data analysis. It uses a series of calculations to first identify the two groups that have the closest association (e.g. whether the gene expression behavior is correlated), and then identify the two groups that have similar associations and merge them until all of the groups are combined into one group. The expression of the selected differential genes was used to calculate the correlation between samples. Cluster analysis of the differentially expressed genes is able to comprehensively and intuitively indicate the relationship and differences between samples. Genes clustered in the same group may have similar biological functions (Fig. 2C and D). A scatter plot of the chip data is frequently used to evaluate the overall distribution of the two groups of data. The raw data analyzed by the chip is standardized and converted into log2, which is drawn in a two-dimensional rectangular coordinate system plane. Each point in the scatter plot represents a probe signal. The X-axis and Y-axis values correspond to the strength of the probe signal in different samples (Fig. 3A and B). The expression profiles indicated that 14 lncRNAs were differentially expressed (fold change ≥1.2, $P<0.05$) in the high and normal glucose groups. Among these, 7 lncRNAs were upregulated and 7 lncRNAs were downregulated in the high glucose group compared to the normal glucose group ($P<0.05$; Table II).

Overview of mRNA profiles in the angiogenic pathway. In total, 22 mRNAs were determined to be differentially expressed in the high vs. normal glucose groups, including 9 upregulated mRNAs and 13 downregulated mRNAs (Table III, Figs. 2D and 3B).

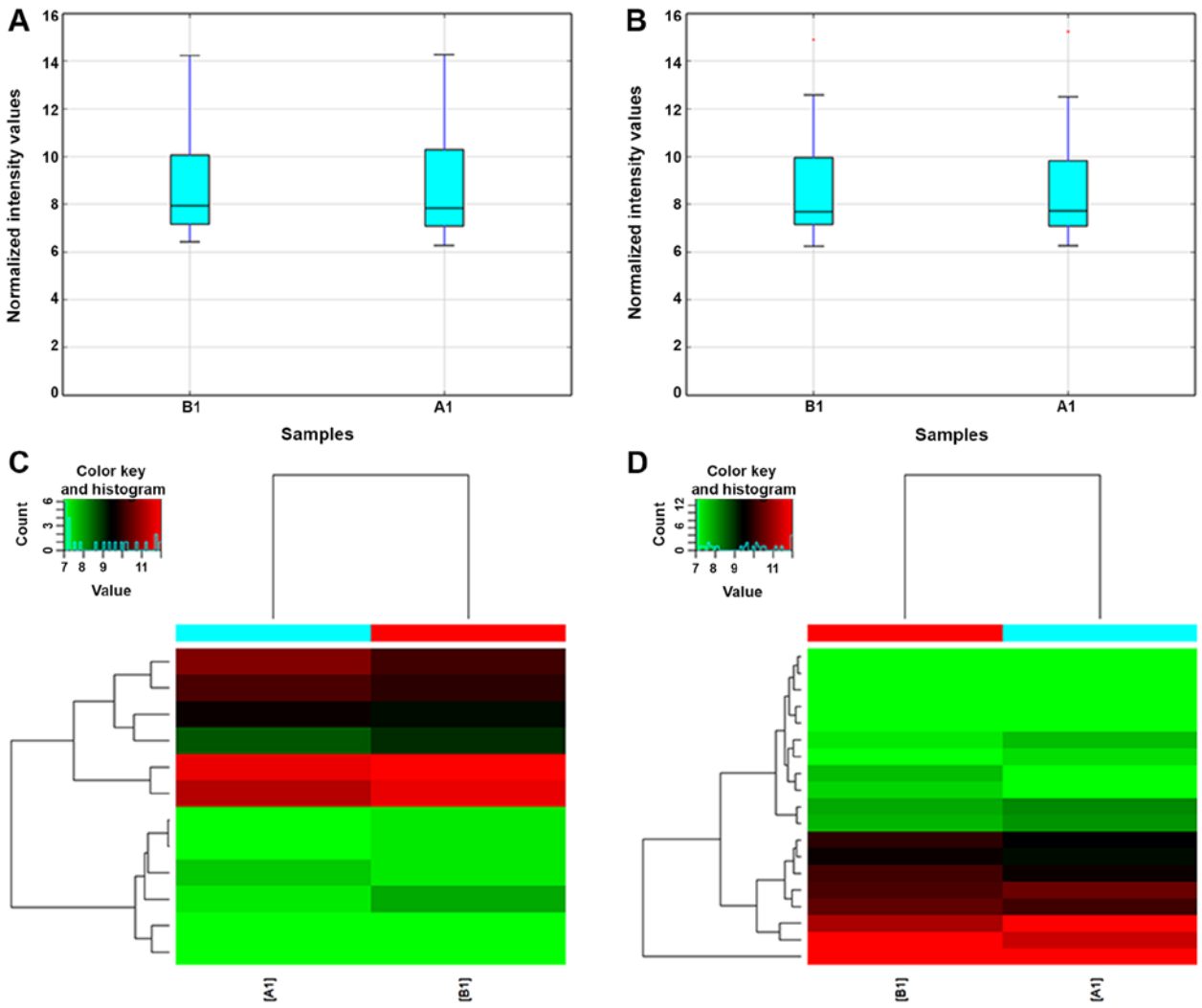

Figure 2. Box plot and hierarchical clustering of lncRNAs and mRNAs. (A) Box plot of lncRNAs; (B) box plot of mRNAs. Data are presented as the mean ± standard deviation. (C) Hierarchical clustering of lncRNAs; (D) hierarchical clustering of mRNAs. A1 represents human skin fibroblasts cultured in conditioned medium with 50 mM glucose as the experimental group; B1 represents human skin fibroblasts cultured in conditioned medium with 5.5 mM glucose as the control group. lncRNA, long non-coding RNA.

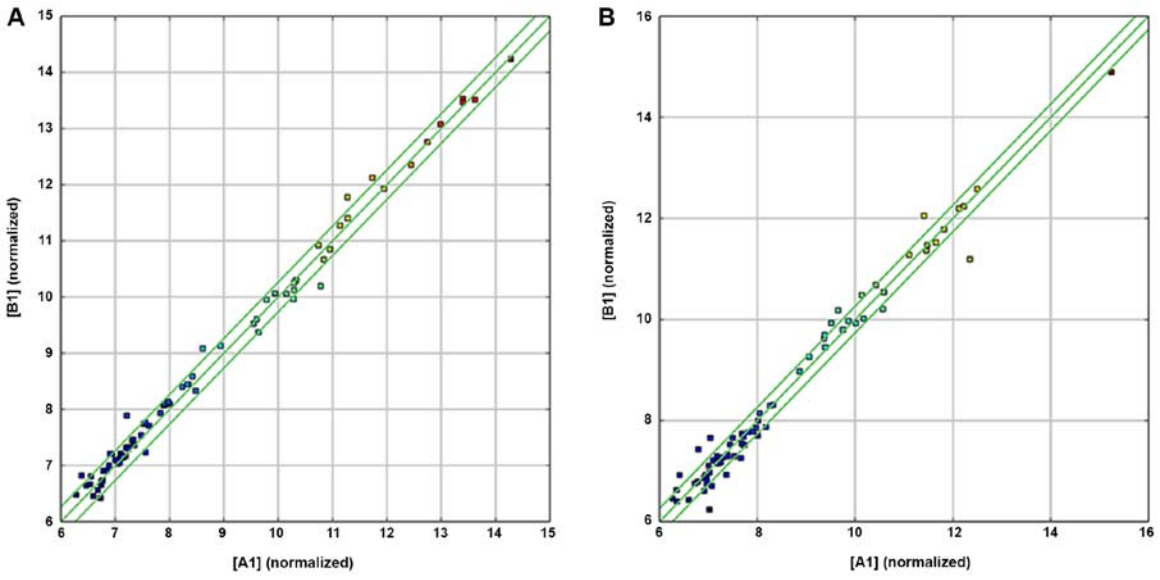

Figure 3. (A) Scatter plot of long non-coding RNAs; (B) Scatter plot of mRNAs. A1 represents human skin fibroblasts cultured in conditioned medium with 50 mM glucose as the experimental group; B1 represents human skin fibroblasts cultured in conditioned medium with 5.5 mM glucose as the control group. The green line represents the threshold line for fold change between the experimental group and control group. Each dot represents a gene.

Table II. Differentially expressed angiogenesis pathway-associated long non-coding RNAs in human skin fibroblasts under high vs. normal glucose conditions.

Seqname	Probe ID	Fold change	Direction of regulation
ENST00000487582	ASPWP0001058	1.2074108	Up
ENST00000560769	ASPWP0002798	1.3577658	Up
ENST00000279573	ASPWP0007625	1.5992882	Up
uc009viz.2	ASPWP0008050	1.2333524	Up
AF080092	ASPWP0008612	1.4161263	Up
ENST00000447329	ASPWP0233858	1.3118266	Up
TCONS_00020502	ASPWP0242229	1.3868367	Up
ENST00000438325	ASPWP0006381	-1.5034269	Down
ENST00000503199	ASPWP0007394	-1.2359937	Down
ENST00000377951	ASPWP0099869	-1.2420934	Down
ENST00000447355	ASPWP0131110	-1.2034646	Down
ENST00000380194	ASPWP0181987	-1.2499400	Down
ENST00000407916	ASPWP0171081	-1.225475	Down
ENST00000534518	ASPWP0089206	-1.2235197	Down

Table III. Differentially expressed angiogenesis pathway-associated mRNAs in human skin fibroblasts under high vs. normal glucose conditions.

Seqname	Probe ID	Fold change	Direction of regulation
NM_002982	ASPWP0003551	1.4274665	Up
NM_002006	ASPWP0005206	1.2722540	Up
NM_170744	ASPWP0006739	1.4474682	Up
NM_021219	ASPWP0008287	1.5533651	Up
NM_002982	ASPWP0009471	1.5335374	Up
NM_003256	ASPWP0010787	1.2091137	Up
NM_002006	ASPWP0010964	1.3310729	Up
ENST00000367976	ASPWP0011091	1.5619674	Up
NM_006153	ASPWP0011949	1.2470495	Up
NM_000899	ASPWP0000190	-1.2406115	Down
NM_002422	ASPWP0001242	-2.2271753	Down
NM_001511	ASPWP0005163	-1.2857458	Down
NM_001305	ASPWP0008354	-1.7152201	Down
NM_005228	ASPWP0009560	-1.2898507	Down
NM_000321	ASPWP0010047	-1.3559353	Down
NM_002659	ASPWP0010442	-1.2347152	Down
NM_001278	ASPWP0011456	-1.2372123	Down
NM_002422	ASPWP0011539	-1.2705653	Down
NM_001143818	ASPWP0011670	-1.3228819	Down
NM_002576	ASPWP0009278	-1.23502	Down
NM_003377	ASPWP0012308	-1.2222489	Down
NM_000602	ASPWP0000680	-1.2365507	Down

RT-qPCR validation. Certain differentially expressed lncRNAs (RP4-791C19.1 and CTD-2589O24.1) and mRNAs [vascular endothelial growth factor B (VEGFB), KIT ligand (KITLG) and serpin family E member 1 (SERPINE1)] were selected to validate the microarray results by RT-qPCR using the $2^{-\Delta\Delta Cq}$ method with GAPDH as the reference gene. The results suggested that the PCR results were consistent with the microarray data (Fig. 4).

Analysis of lncRNAs and their protein-coding gene targets in the angiogenic pathway. Various angiogenic pathway-associated lncRNAs were predicted to regulate the

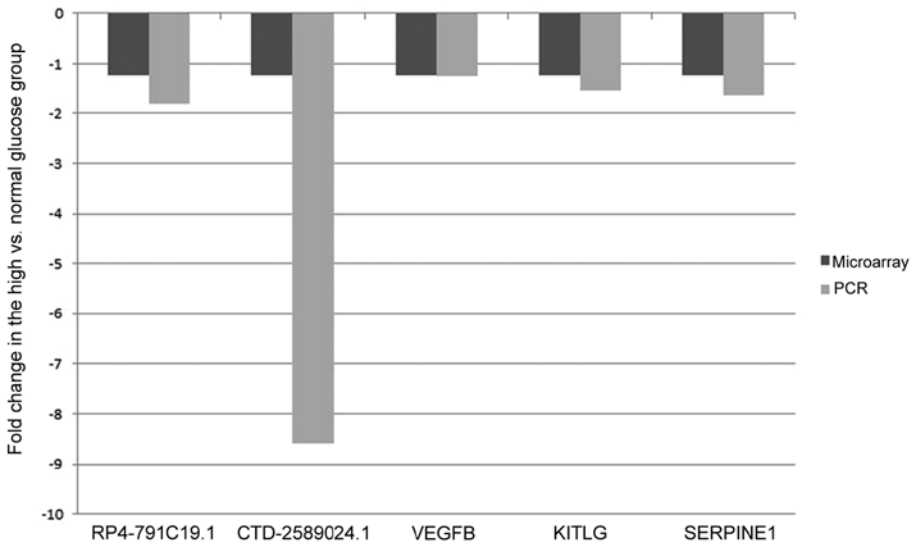

Figure 4. Validation of differentially expressed RNAs according to microarray by RT-qPCR. RP4-791C19.1, CTD-2589O24.1, VEGFB, KITLG, SERPINE1 determined to be differentially expressed under high-glucose conditions compared with normal-glucose conditions by microarray were validated by RT-qPCR. It was indicated that the microarray data were in agreement with the RT-qPCR results. RT-qPCR, reverse transcription-quantitative PCR; VEGFB, vascular endothelial growth factor B; KITLG, KIT ligand; SERPINE1, serpin family E member 1.

RNA expression in the high-glucose group (Table IV). It was indicated that the downregulated lncRNAs (RP4-791C19.1 and CTD-2589O24.1) may act on their target gene epidermal growth factor receptor (EGFR) and p21 (RAC1) activated kinase 1 (PAK1), respectively, as enhancers and cis-regulate their expression under high-glucose conditions.

Discussion

The present study provides novel insight into the molecular mechanisms of wound healing in diabetes mellitus. Angiogenesis is the process of new capillary formation (13), which involves multiple stages, including endothelial cell proliferation, migration, tube formation, micro-vessel development and branching, as well as tissue remodeling (14). Angiogenesis is a highly regulated process that supplies cells with the nutrients and gases through blood vessels required for wound healing (15). Impaired wound healing is one of the major complications of diabetes that increases morbidity, mortality and health expenditure (16). Therefore, it is necessary to gain a more in-depth understanding of the molecular mechanisms of wound healing in diabetes to identify appropriate treatment modalities and promote wound healing.

Angiogenic imbalance contributes to difficulty in wound healing in patients with diabetes (17). It has been indicated that lncRNAs, which are a class of non-coding RNAs longer than 200 nucleotides and localized in the nucleus or cytoplasm, are involved in different regulatory mechanisms, including chromatin remodeling, protein scaffolding and translational control (18). Long non-coding RNAs have emerged as the critical regulators of angiogenesis in various diseases. For instance, a knockout strategy suggested a functional role of the lncRNA Fendrr to interfere with chromatin modifications and thereby developmental signaling in the heart (19). The lncRNA associated with microvascular invasion in hepatocellular carcinoma promotes angiogenesis, and lncRNA MVIH serves as a predictor of poor recurrence-free survival following hepatectomy (20). However, the functions of angiogenesis pathway-associated lncRNAs in the mechanisms of wound healing in patients with diabetes have remained largely elusive.

Effects of high glucose on the biological behavior of fibroblasts have been previously reported in the literature. Buranasin *et al* (21) indicated that fibroblast migration was significantly inhibited in cells cultured at higher glucose levels (50 mM), resulting in prolonged wound closure; cell proliferation at 50 mM glucose was significantly reduced compared with that in the control group (5.5 mM). Similarly, in the present study, higher glucose levels (50 mM) were used as the experimental group to mimic a diabetic environment *in vitro* and was used together with a control group with normal glucose levels (5.5 mM) to examine the angiogenesis pathway-associated lncRNA expression profiles in the high and normal glucose groups. Analysis of the microarray data suggested that 14 angiogenesis pathway-associated lncRNAs and 22 mRNAs were differentially expressed between the two groups. Among these, 7 lncRNAs and 9 mRNAs were indicated to be upregulated and 7 lncRNAs and 13 mRNAs were downregulated in the high glucose group compared to the normal glucose group. Several candidate angiogenesis pathway-associated lncRNAs (RP4-791C19.1 and CTD-2589O24.1) and mRNAs (VEGFB, KITLG and SERPINE1) were verified by RT-qPCR and the results were consistent with the microarray data, implying that the results of the microarray were reliable.

In the present study, the angiogenesis pathway-associated lncRNAs RP4-791C19.1 and CTD-2589O24.1 were identified to be downregulated in the high-glucose group, and the also associated mRNAs EGFR and PAK1 were also downregulated in the high-glucose group. Their differential expression changed in the same direction. Furthermore, as respective potential target genes of lncRNAs RP4-791C19.1 and CTD-2589O24.1, EGFR and PAK1 were identified. To detect the functions of the lncRNAs, the GENCODE

Table IV. Genes whose mRNA expression was predicted to be regulated by angiogenesis pathway-associated long non-coding RNAs under high-glucose conditions.

Gene symbol	Direction of regulation	Genomic relationship	mRNA symbol
XLOC_009823	Up	Downstream	KITLG
CTD-2589O24.1	Down	Downstream	PAK1
RP11-350N15.4	Up	Overlapping	FGFR1
RP11-395B7.7	Up	Downstream	SERPINE1
RP4-791C19.1	Down	Downstream	EGFR

VEGFB, vascular endothelial growth factor B; KITLG, KIT ligand; SERPINE1, serpin family E member 1; FGFR1, fibroblast growth factor receptor 1; EGFR, epidermal growth factor receptor; PAC1, p21 (RAC1) activated kinase 1.

annotation was used. In addition, the UCSC Genome Browser was used to predict the associations of and mechanisms regulating the lncRNAs and the angiogenesis pathway-associated target genes.

Of note, lncRNAs RP4-791C19.1 and CTD-2589O24.1 transcribed from chromosome 7 and 11, respectively, were indicated to act as enhancers to regulate their neighboring protein-coding genes. Enhancers are frequently defined as cis-acting DNA sequences that increase gene transcription. They generally function independently of the direction and distance from their target promoters (22). Enhancer-like lncRNAs may activate proximal promoters and stimulate the transcription of their nearby coding genes (23). Accumulating evidence indicates that depletion of enhancer-like lncRNAs may lead to decreased expression of their nearby coding genes (24). It may therefore be hypothesized that downregulation of the angiogenesis pathway-associated lncRNAs RP4-791C19 and CTD-2589O24.1 may lead to decreased expression of their associated genes, EGFR and PAK1, respectively. Accumulating evidence has also demonstrated that EGFR and PAK1 participate in new capillary blood vessel formation and have a critical role in angiogenesis. For instance, upregulation of EGFR leads to poor survival through the activation of angiogenesis in glioblastoma (25). Effective inhibition of EGFR activation was indicated to ameliorate gastric tumor development through a delay in growth, induction of apoptosis, as well as inhibition of metastasis and angiogenesis (26). PAK1 is the best-characterized member of an evolutionarily conserved family of serine/threonine kinases, which has a key role in the regulation of cell morphogenesis, motility, mitosis and angiogenesis (27).

There are several limitations to this study. First, the functions of the differentially expressed angiogenesis pathway-associated lncRNAs under high-glucose conditions were predicted but the exact functional roles of these lncRNAs were not verified and illustrated. Analysis of the potential gene targets of the lncRNAs implicated in human angiogenesis pathways demonstrated that lncRNAs RP4-791C19.1 and CTD-2589O24.1 may act on their target genes, EFGR and PAK1, respectively, as enhancers and cis-regulate their expression. As the next step, the detailed functional roles and underlying regulatory mechanisms of these lncRNAs in the angiogenesis signaling pathway should be illustrated. In future research, the functions of the identified lncRNAs may be investigated by overexpression and RNA interference methods *in vivo* or *in vitro*. As another limitation, cell motility, the cell cycle and proliferation were not assessed at higher concentrations of glucose in the present study. Dermal fibroblasts have essential roles in wound healing. However, they lose their normal regenerative functions under certain pathologic conditions, e.g. in chronic diabetic wounds (28). In the present study, high-glucose conditions mimicking the diabetic environment, as well as a low glucose concentration resembling the normal physiological environment were used. Culture under high-glucose conditions may reduce the angiogenic potential of dermal fibroblasts, which may explain for the mechanism of diabetic wound healing from the perspective of vascularization. However, skin-derived fibroblasts represent a part of angiogenetic processes and endothelial cells are also involved. In future studies, differentially expressed angiogenesis pathway-associated lncRNAs in endothelial cells under high-glucose conditions should also be investigated. In recent years, high-glucose conditions were used to mimic the diabetic environment [e.g., Duru *et al* (29)]; however, wound-healing in a diabetic patient is far more complex than just a hyperglycemic micro-environment. It involves continuous inflammation and chronic capillary damage (30). In further research, factors including a hyperglycemic microenvironment, inflammatory agents and chronic capillary damage will be combined to mimic a diabetic environment. As another limitation, there may be differences between *in vivo* and *in vitro* experiments. Therefore, further studies in animal models, e.g. a streptozotocin-induced rat model of diabetes, may be required to confirm the roles of these differentially expressed angiogenesis pathway-associated lncRNAs in wound healing *in vivo*. In the future, these lncRNAs may serve as novel therapeutic targets for the treatment of wounds in patients with diabetes in routine clinical practice.

In conclusion, in the present study, 14 angiogenesis pathway-associated lncRNAs and 22 mRNAs were identified to be differentially expressed under high-glucose conditions. Among them, the downregulated lncRNAs RP4-791C19.1 and CTD-2589O24.1 may act on their respective target genes EGFR and PAK1 as enhancers and cis-regulate their expression. In the future, it is necessary to confirm and illustrate the detailed functional roles and underlying regulatory mechanisms of these lncRNAs in the angiogenesis signaling pathway to provide new directions to promote wound healing in diabetes.

Acknowledgements

Not applicable.

Funding

The current study was supported by the Chinese National Natural Science Foundation (grant nos. 81860340 and 81460293), the Special Fund for Graduate Innovation Project of Nanchang University (grant no. CX2017249) and the Special Fund for Graduate Innovation Project of Jiangxi province (grant no. YC2019-B019).

Availability of data and materials

All data generated or analyzed during this study are included in this published article.

Authors' contributions

LT performed the experiments and wrote the manuscript. QH and YH analyzed data and edited the manuscript. DL designed the experiment and revised the manuscript. All authors have read and approved the final version of the manuscript.

Ethics approval and consent to participate

The present study was approved by the Biomedical Ethics Committee of the Affiliated Hospital of Nanchang University. All patients provided informed written consent.

Patient consent for publication

Not applicable.

Competing interests

The authors declare that they have no competing interests.

References

1. Hu C and Jia W: Diabetes in China: Epidemiology and genetic risk factors and their clinical utility in personalized medication. Diabetes 67: 3-11, 2018.
2. Tellechea A, Leal EC, Kafanas A, Auster ME, Kuchibhotla S, Ostrovsky Y, Tecilazich F, Baltzis D, Zheng Y, Carvalho E, *et al*: Mast cells regulate wound healing in diabetes. Diabetes 65: 2006-2019, 2016.
3. Davidson EP, Coppey LJ, Shevalye H, Obrosov A and Yorek MA: Vascular and neural complications in type 2 diabetic rats: Improvement by sacubitril/valsartan greater than valsartan alone. Diabetes 67: 1616-1626, 2018.
4. Mercer TR, Dinger ME and Mattick JS: Long non-coding RNAs: Insights into functions. Nat Rev Genet 10: 155-159, 2009.
5. Herter EK and Xu LN: Non-coding RNAs: New players in skin wound healing. Adv Wound Care (New Rochelle) 6: 93-107, 2017.
6. Cai B, Zheng Y, Ma S, Ma S, Xing Q, Wang X, Yang B, Yin G and Guan F: Long noncoding RNA regulates hair follicle stem cell proliferation and differentiation through PI3K/AKT signal pathway. Mol Med Rep 17: 5477-5483, 2018.
7. Chen L, Li J, Li Q, Li X, Gao Y, Hua X, Zhou B and Li J: Overexpression of LncRNA AC067945.2 down-regulates collagen expression in skin fibroblasts and possibly correlates with the VEGF and Wnt signalling pathways. Cell Physiol Biochem 45: 761-771, 2018.
8. Guo L, Huang X, Liang P, Zhang P, Zhang M, Ren L, Zeng J, Cui X and Huang X: Role of XIST/miR-29a/LIN28A pathway in denatured dermis and human skin fibroblasts (HSFs) after thermal injury. J Cell Biochem 119: 1463-1474, 2018.
9. Kumar MM and Goyal R: LncRNA as a therapeutic target for angiogenesis. Curr Top Med Chem 17: 1750-1757, 2017.
10. Harrow J, Denoeud F, Frankish A, Reymond A, Chen CK, Chrast J, Lagarde J, Gilbert JGR, Storey R, Swarbreck D, *et al*: GENCODE: Producing a reference annotation for ENCODE. Genome Biol 7 (Suppl 1): S4.1-S9, 2006.
11. Schmittgen TD and Livak KJ: Analyzing real-time PCR data by the comparative C(T) method. Nat Protoc 3: 1101-1108, 2008.
12. Wilfinger WW, Mackey K and Chomczynski P: Effect of pH and ionic strength on the spectrophotometric assessment of nucleic acid purity. Biotechniques 22: 474-476, 478-481, 1997.
13. Nambiar DK, Kujur PK and Singh RP: Angiogenesis assays. Methods Mol Biol 1379: 107-115, 2016.
14. Potente M, Gerhardt H and Carmeliet P: Basic and therapeutic aspects of angiogenesis. Cell 146: 873-887, 2011.
15. Martin P and Nunan R: Cellular and molecular mechanisms of repair in acute and chronic wound healing. Br J Dermatol 173: 370-378, 2015.
16. Dong Y, Rodrigues M, Kwon SH, Li X, Sigen A, Brett EA, Elvassore N, Wang W and Gurtner GC: Acceleration of diabetic wound regeneration using an in situ-formed stem-cell-based skin substitute. Adv Healthc Mater 7: e1800432, 2018.
17. Wang W, Yan X, Lin Y, Ge H and Tan Q: Wnt7a promotes wound healing by regulation of angiogenesis and inflammation: Issues on diabetes and obesity. J Dermatol Sci 2018 (Online ahead of print).
18. Mercer TR and Mattick JS: Structure and function of long noncoding RNAs in epigenetic regulation. Nat Struct Mol Biol 20: 300-307, 2013.
19. Klattenhoff CA, Scheuermann JC, Surface LE, Bradley RK, Fields PA, Steinhauser ML, Ding H, Butty VL, Torrey L, Haas S, *et al*: Braveheart, a long noncoding RNA required for cardiovascular lineage commitment. Cell 152: 570-583, 2013.
20. Yuan SX, Yang F, Yang Y, Tao QF, Zhang J, Huang G, Yang Y, Wang RY, Yang S, Huo XS, *et al*: Long noncoding RNA associated with microvascular invasion in hepatocellular carcinoma promotes angiogenesis and serves as a predictor for hepatocellular carcinoma patients' poor recurrence-free survival after hepatectomy. Hepatology 56: 2231-2241, 2012.
21. Buranasin P, Mizutani K, Iwasaki K, Mahasarakham CPN, Kido D, Takeda K and Izumi Y: High glucose-induced oxidative stress impairs proliferation and migration of human gingival fibroblasts. PLoS One 13: e201855, 2018.
22. Pennacchio LA, Bickmore W, Dean A, Nobrega MA and Bejerano G: Enhancers: Five essential questions. Nat Rev Genet 14: 288-295, 2013.
23. Ørom UA, Derrien T, Beringer M, Gumireddy K, Gardini A, Bussotti G, Lai F, Zytnicki M, Notredame C, Huang Q, *et al*: Long noncoding RNAs with enhancer-like function in human cells. Cell 143: 46-58, 2010.
24. Lai F, Orom UA, Cesaroni M, Beringer M, Taatjes DJ, Blobel GA and Shiekhattar R: Activating RNAs associate with Mediator to enhance chromatin architecture and transcription. Nature 494: 497-501, 2013.
25. Ngo MT and Harley B: Perivascular signals alter global gene expression profile of glioblastoma and response to temozolomide in a gelatin hydrogel. Biomaterials 198: 122-134, 2018.
26. Wu Y, Yuan M, Su W, Zhu M, Yao X, Wang Y, Qian H, Jiang L, Tao Y, Wu M, *et al*: The constitutively active PKG II mutant effectively inhibits gastric cancer development via a blockade of EGF/EGFR-associated signalling cascades. Ther Adv Med Oncol 10: 1960366675, 2018.
27. Li LH, Wu GY, Lu YZ, Chen XH, Liu BY, Zheng MH and Cai JC: p21-activated protein kinase 1 induces the invasion of gastric cancer cells through c-Jun NH2-terminal kinase-mediated activation of matrix metalloproteinase-2. Oncol Rep 38: 193-200, 2017.
28. Jung N, Yu J, Um J, Dubon MJ and Park KS: Substance P modulates properties of normal and diabetic dermal fibroblasts. Tissue Eng Regen Med 13: 155-161, 2016.
29. Duru EA, Fu Y and Davies MG: Role of S-1-P receptors and human vascular smooth muscle cell migration in diabetes and metabolic syndrome. J Surg Res 177: e75-e82, 2012.
30. Zhao R, Liang H, Clarke E, Jackson C and Xue M: Inflammation in chronic wounds. Int J Mol Sci 17: 2085, 2016.